Diagnosis of PEM Fuel Cells through Current Interruption

M.A. Rubio *, A. Urquia, S. Dormido

Dept. Informática y Automática, ETS Ingeniería Informática, UNED

Juan del Rosal 16, 28040 Madrid, Spain

Abstract

Electrochemical Impedance Spectroscopy (EIS) is widely used for the characterization of PEM fuel cells. In particular, EIS data is used for parameter estimation of the PEMFC equivalent circuit model. However, EIS exhibits some practical limitations when it is applied to the in-field diagnosis and control of fuel cells (e.g., the equipment's size, weight and cost). An alternative methodology for the parameter estimation of the PEMFC equivalent circuit is proposed. Firstly, the cell's transient response after current interruption is experimentally measured. The equipment required to perform this experiment is easily portable and inexpensive. Secondly, the cell equivalent circuit parameters are estimated by fitting the cell's experimental data to the analytical expression of the cell model transient response after current interruption. The application of this cell assessment methodology is illustrated by means of a case study: the diagnosis of the cathode flooding in a PEM fuel cell.

Key words: Diagnosis, Impedance spectroscopy, Current interruption, Flooding

PACS:

* Corresponding author.

Email addresses: marubio@dia.uned.es (M.A. Rubio), aurquia@dia.uned.es

1 Introduction

Our society is suffering from fossil fuel shortage. Fossil fuels (i.e, coal, oil, and natural gas) also contribute to a number of environmental problems during their extraction, transportation, and use. In particular, their use to obtain energy generates emissions that contribute to global warming and climate change. As an alternative, fuel cells are one of the most promising means of producing energy.

A considerable research effort has been made in order to understand the physical and chemical phenomena involved in the PEMFC operation. Numerous mathematical models, describing these phenomena with great precision, have been proposed [1–7].

Also, PEMFC models with low computational cost, suited for use in control applications, have been developed. In particular, Randles electric models are frequently used. In this context, EIS techniques are employed to study the fuel cell behavior, and to estimate the value of the cell model parameters. However, EIS equipment is too expensive and bulky for use on in-field assessment of operating commercial cells [8–14]. As a consequence, this approach to PEMFC modelling is not suited for in-field control applications.

1.1 Contributions of this paper

An alternative methodology for PEMFC diagnosis, intended to be used for control applications, is proposed in this manuscript. Instead of using EIS, the

(A. Urquia), `sdormido@dia.uned.es` (S. Dormido).

cell model parameters are identified from the cell response after current interruption (CI). The advantage of this approach is that the equipment required to perform the CI experiments is inexpensive and easily portable.

The CI data is used to estimate the parameters of a Randles electric model. This PEMFC model has been specially formulated in order to facilitate the parameter estimation from CI data. The simplified randles model of the PEMFC and the proposed parameter estimation method are discussed.

The use of CI techniques for cell state characterization is not new. Some cell diagnosis methods, based on the CI technique, have been proposed by other authors. In particular, CI techniques can be successfully applied to the estimation of the FC resistance [15]. Other methods, based on the analysis of the cell response after a step change in the load, are used to validate the data obtained from the EIS study [16].

As a difference with other authors' methods, the proposed methodology allows estimating the significant operation parameters of the PEMFC only from the CI data. Rich information about the cell dynamic behavior is contained in the cell response to step and impulse inputs. In this case, the information is extracted from the cell response after CI. The impulse has a wide spectrum of frequencies, exciting the FC fundamental phenomena [17–19].

The manuscript has been structured into seven sections and two appendices. Firstly, a Randles electric model commonly used to represent the PEMFC dynamic behavior is discussed (Section 2). Then, a simplified model of the Warburg impedance is proposed (Section 3). It allows writing the cell impedance as an analytical expression, in terms of the cell fundamental physical parameters (Section 4). This analytical expression of the cell impedance is

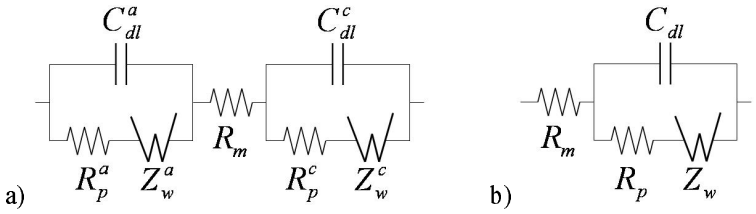

Fig. 1. PEMFC electric models: a) complete model; b) simplified model.

used to obtain the analytical expression of the PEMFC voltage after CI (Section 5). The cell model parameters can be estimated by fitting the analytical expression of the cell voltage after CI to the CI experimental data (Section 6). Finally, the proposed methodology is applied to a case study: the diagnosis of the cathode flooding in a PEMFC (Section 7).

2 Equivalent circuit for a PEMFC

The voltage drop across the fuel cell (V_{cell}) can be written as a function of the over-voltages of the anode (η_a), the cathode (η_c) and the membrane (η_m) [15,20]:

$$V_{cell} = E_{oc} - \eta_a - \eta_m - \eta_c \tag{1}$$

The cell voltage in Eq. (1) can be modelled by the electric circuit shown in Fig. 1a, which is composed of Randles models connected in series [16,8]. Z^a_W and Z^c_W are the Warburg impedances associated to the gas diffusion in the anode and the cathode respectively. R^a_p and R^c_p are the charge transfer resistances in the anode and the cathode. C^a_{dl} and C^c_{dl} are the double layer capacities in the anode and the cathode. Finally, R_m is the membrane resistance.

Two additional hypotheses are made in order to simplify the cell model shown in Fig. 1a. As a result, the simplified model shown in Fig. 1b is obtained.

(1) The oxygen reduction reaction in the cathode in very slow in comparison with the hydrogen oxidation reaction [21,22]. Therefore, the anode over-voltage is very small in comparison with the cathode over-voltage. As a consequence, the anode over-voltage contribution to the cell voltage can be neglected in the model.

(2) The double layer capacity, which is usually represented by constant-phase elements, is represented by a pure, single-frequency theoretical capacity [9,14,16,23].

3 Modelling of the Warburg impedance

The Warburg impedance (Z_W) can be written in the Laplace domain as a function of the finite length diffusion [8]:

$$Z_W(s) = R_d \frac{\tanh \sqrt{s\tau_d}}{\sqrt{s\tau_d}} \tag{2}$$

where the diffusion resistance (R_d) and the diffusion time constant (τ_d) can be calculated from the following expressions:

$$R_d = \frac{RT\delta}{SC_g Dn^2F^2} \tag{3}$$

$$\tau_d = \frac{\delta^2}{D} \tag{4}$$

The following approximation of the Warburg impedance in Eq. (2) is proposed:

$$Z_W(s) = \frac{R_1^*}{1 + R_1^* C_1^* s} + \frac{R_2^*}{1 + R_2^* C_2^* s} \tag{5}$$

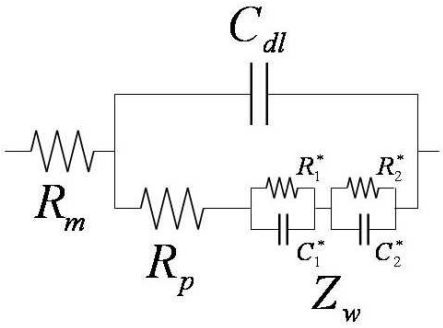

Fig. 2. PEMFC electric model with Warburg impedance calculated from Eq. (5).

where

$$R_i^* = R_i R_d \qquad \text{for } i = \{1, 2\} \tag{6}$$

$$C_i^* = C_i \frac{\tau_d}{R_d} \qquad \text{for } i = \{1, 2\} \tag{7}$$

or, equivalently

$$Z_W(s) = R_d \left(\frac{R_1}{1 + R_1 C_1 \tau_d s} + \frac{R_2}{1 + R_2 C_2 \tau_d s} \right) \tag{8}$$

This approximation is equivalent to model the cell by using the circuit shown in Fig. 2. Four new parameters have been introduced in Eq. (8): R_1, R_2, C_1 and C_2. The values of these four parameters are calculated by fitting Eq. (8) to Eq. (2) in the frequency range from $2 \cdot 10^{-1} s^{-1}$ to $1.5 \cdot 10^{3} s^{-1}$, considering $\tau_d = 1$. The calculated values are shown in Table 1.

Table 1

Fitted values of the parameters in Eq. (8).

Parameter	R_1 (Ω)	R_2 (Ω)	C_1 (F)	C_2 (F)
Value	0.8463	0.1033	0.3550	0.03145

The exact value of the impedance, calculated from Eq. (2), and the approximated value, obtained from Eq. (8) using the previously calculated values of

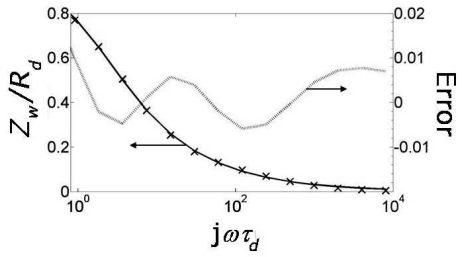

Fig. 3. Exact (−) and approximated (×) Warburg impedances. Absolute error.

R_1, R_2, C_1 and C_2, are plotted in Fig. 3. Also, the absolute error is shown in Fig. 3.

4 Modelling of the PEMFC impedance

The cell impedance (Z_{cell}), calculated from the circuit shown in Fig. 2, is the following:

$$Z_{cell}(s) = \frac{as^2 + bs + c}{ds^3 + es^2 + fs + g} \tag{9}$$

where the parameters a, b, c, d, e, f and g can be calculated from the following expressions:

$$a = 9.76 \cdot 10^{-4} R_p \tau_d^2 \tag{10}$$
$$b = 0.304 R_p \tau_d + 3.38 \cdot 10^{-2} R_d \tau_d \tag{11}$$
$$c = R_p + 0.949 R_d \tag{12}$$
$$d = 9.76 \cdot 10^{-4} C_{dl} R_p \tau_d^2 \tag{13}$$
$$e = 3.37 \cdot 10^{-2} C_{dl} R_d \tau_d + 0.3048 C_{dl} R_p \tau_d + 9.76 \cdot 10^{-4} \tau_d^2 \tag{14}$$
$$f = C_{dl} R_p + 0.3048 \tau_d + 0.949 C_{dl} R_d \tag{15}$$
$$g = 1 \tag{16}$$

The cell impedance described by Eq. (9) depends on the following four physical parameters: C_{dl}, R_d, R_p and τ_d. As it will be discussed later, the value of these parameters can be estimated from the cell response after CI.

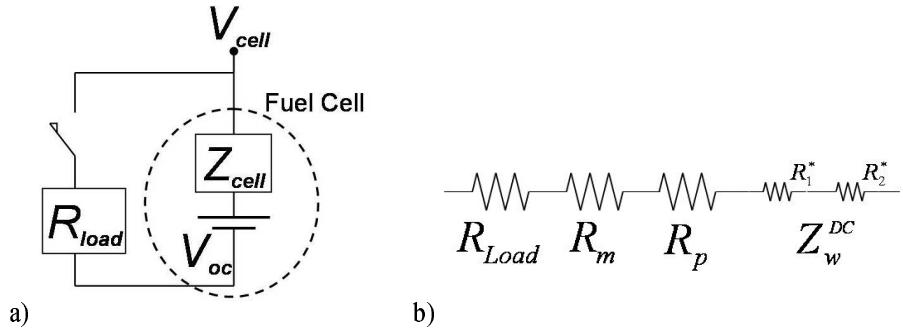

Fig. 4. CI experimental setup: a) equivalent circuit; b) DC impedance (Z_T).

5 PEMFC response after CI

The simplified model of the Warburg impedance proposed in Section 3 has been used (in Section 4) to obtain an analytical expression of the cell impedance. Now, this analytical expression of the cell impedance will be used to obtain an analytical expression for the PEMFC voltage response after CI.

The equivalent circuit of the CI experimental setup is shown in Fig. 4a. The load impedance is R_{load}. The cell impedance (Z_{cell}) is calculated from Eq. (9). As the cell impedance has only real poles, the cell response after CI is equal to the cell response after a current impulse at $t = 0$ (see Appendix A):

$$I(t) = I_0 \delta(t) \tag{17}$$

where $\delta(t)$ is the Dirac delta, and I_0 is the steady-state value of the current at $t = 0^-$. It is calculated as follows:

$$I_0 = \frac{V_{cell}(t = 0^-)}{Z_T(t = 0^-)} \tag{18}$$

where Z_T is the DC impedance of the circuit shown in Fig. 4a. The equivalent circuit of the impedance Z_T is represented in Fig. 4b.

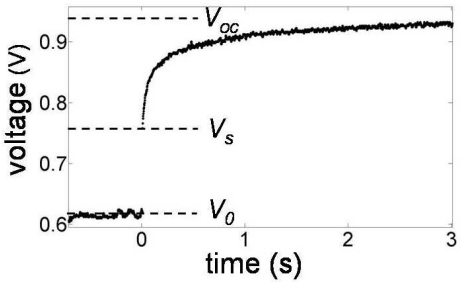

Fig. 5. Experimental data of the cell voltage after CI.

The cell voltage can be written, in the Laplace domain, as follows:

$$V_{cell}(s) = V_{oc} - Z_{cell}(s)I(s) \tag{19}$$

The time-domain expression of the cell impedance proposed in Section 4 is the following:

$$L^{-1}\left[Z_{cell}(s)\right] = R_m\delta(t) + \sum_{i=1}^{3}\left(\frac{ar_i^2 + br_i + c}{3dr_i^2 + 2er_i + f}\right)e^{-r_i t} \tag{20}$$

where r_1, r_2 and r_3 are the three roots of the polynomial $ds^3 + es^2 + fs + g$.

The dynamic response of the cell voltage after CI is the following:

$$V_{cell}(t) = V_{oc} - I_0\left(R_m\frac{1}{\sigma\sqrt{2\pi}}e^{-t^2/2\sigma^2} + \alpha_1 e^{-r_1 t} + \alpha_2 e^{-r_2 t} + \alpha_3 e^{-r_3 t}\right) \tag{21}$$

where

$$\alpha_i = \frac{ar_i^2 + br_i + c}{3dr_i^2 + 2er_i + f} \qquad \text{for } i = 1, 2, 3 \tag{22}$$

and also, it must be satisfied:

$$\int_{-\infty}^{\infty}\frac{1}{\sigma\sqrt{2\pi}}e^{-t^2/2\sigma^2}dt = 1 \tag{23}$$

The parameter σ can be estimated from the CI experimental data as follows.

The CI experimental data allow estimating the over-voltage due to the membrane resistance [24,15]. It corresponds to the abrupt rising of the voltage, from V_0 to V_s, at time $t = 0^+$ (see Fig. 5). V_0 is the initial voltage, and V_s is the voltage at $t = 0^+$. Both can be estimated from the CI experimental data. Then, the membrane resistance (R_m) can be calculated from the following expression:

$$V_s - V_0 = I_0 R_m \tag{24}$$

Finally, the dynamic response of the cell voltage can be calculated, for $t > 0^+$ (i.e., for $V_{cell} > V_s$), from the following expression:

$$V_{cell}(t) = V_{oc} - V_s - I_0 \left(\alpha_1 e^{-r_1 t} + \alpha_2 e^{-r_2 t} + \alpha_3 e^{-r_3 t} \right) \tag{25}$$

where V_{oc} is the steady-state, open-circuit voltage of the PEMFC (see Fig. 5).

In order to illustrate the dynamic behavior of the simplified cell model shown in Fig. 2, the cell voltage after CI (calculated from Eq. (25)) and the impedance spectra are plotted in Fig. 6 for selected values of the parameters C_{dl}, R_d, R_p and τ_d.

6 Model parameter estimation from CI data

The voltage after CI of the cell represented by Eq. (9) is described by Eq. (25). The α_i coefficients depend on the roots r_i and on the parameters a, b, c, d, e and f (see Eq. (22)). These parameters depend on the physical parameters C_{dl}, R_d, R_p and τ_d (see Eqs. (10)-(15)). As a consequence, $V_{cell}(t)$ is a function of r_1, r_2, r_3, C_{dl}, R_d, R_p and τ_d.

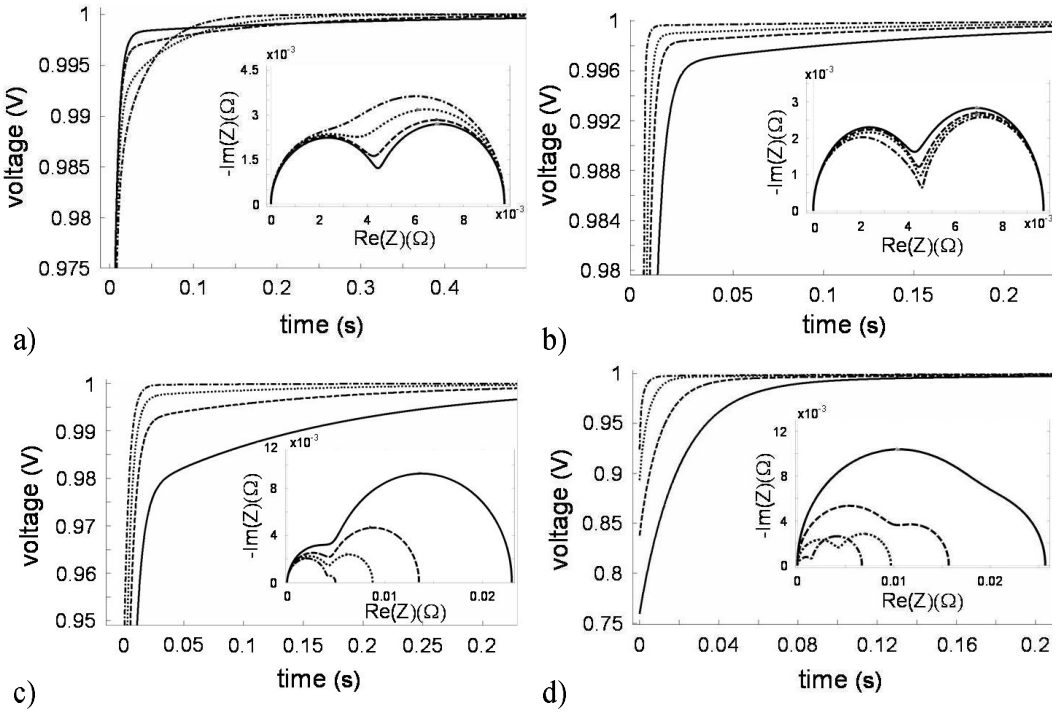

Fig. 6. Simulated cell voltage after CI and impedance spectra for selected parameter values. Baseline: $\tau_d = 0.5s$, $C_{dl} = 0.1F$, $R_d = 6m\Omega$ and $R_p = 4m\Omega$. a) $\tau_d = \{1s(-)$, Baseline $(--)$, $0.2s(...)$, $0.1s(-.-)\}$; b) $C_{dl} = \{$ Baseline (-), $0.5F(--)$, $0.2F(...)$, $0.1F(-.-)\}$; c) $R_d = \{20m\Omega(-)$, $10m\Omega(--)$, Baseline $(...)$, $1m\Omega(-.-)\}$; and d) $R_p = \{20m\Omega(-)$, $10m\Omega(--)$, Baseline $(...)$, $1m\Omega(-.-)\}$.

The analytical expression of $V_{cell}(t)$ as a function of r_1, r_2, r_3, C_{dl}, R_d, R_p and τ_d is obtained by symbolic manipulation of Eqs. (25), (22), and (10)-(15). Finally, in order to estimate the value of these seven parameters (i.e., r_1, r_2, r_3, C_{dl}, R_d, R_p and τ_d), this analytical expression of $V_{cell}(t)$ can be fitted to the experimental data of the cell voltage after CI (for $V_{cell} > V_s$).

The procedure described in this section allows estimating the value of the parameters R_m, C_{dl}, R_d, R_p and τ_d. These parameters completely define the simplified model of the fuel cell shown in Fig. 2.

7 Case study: modelling of the cathode flooding process

Cathode flooding and drying have a relevant effect on the cell performance. In order to study the effect of the cathode flooding on the cell model parameters, the parameter estimation methodology proposed in Section 6 can be repeatedly applied during the flooding process. The data obtained from each CI experiment run, corresponding to a given cathode flooding level, is used to estimate the parameters of the cell electric model shown in Fig. 2.

7.1 Experimental setup

PEMFC characteristics: 25 cm^2 electrode surface; NAFION 112 membrane; electrodes of coal cloth; and double serpentine topology in anode and cathode. *Initial experimental conditions*: 26^0C and 60% relative humidity. *Experimental conditions*: cell temperature is not controlled.

The experiment is conducted as follows. The PEMFC is fed with hydrogen and oxygen at the same pressure: 0.5 bars. The anode and cathode exhausts are kept closed. An electric load of 0.066 Ω is connected. Periodically, CI are performed and an oscilloscope is used for cell voltage reading, with a sample period of 2 ms.

In order to study the effect of the cathode flooding on the cell voltage and current, a data acquisition card is used to record the cell voltage, with a sample period of 1 s. This experimental data is used to estimate the amount of water produced in the reaction.

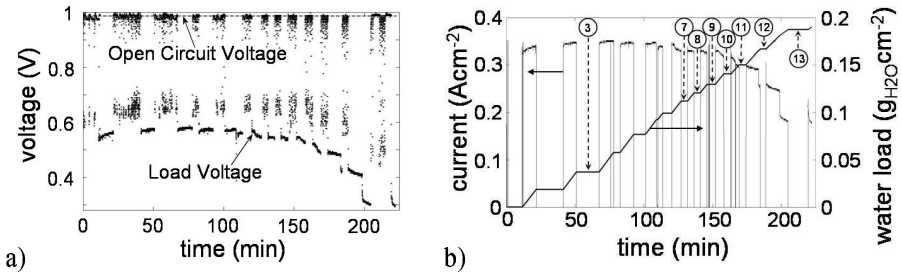

Fig. 7. Overall experiment results: a) cell voltage; b) cell current and estimated amount of water.

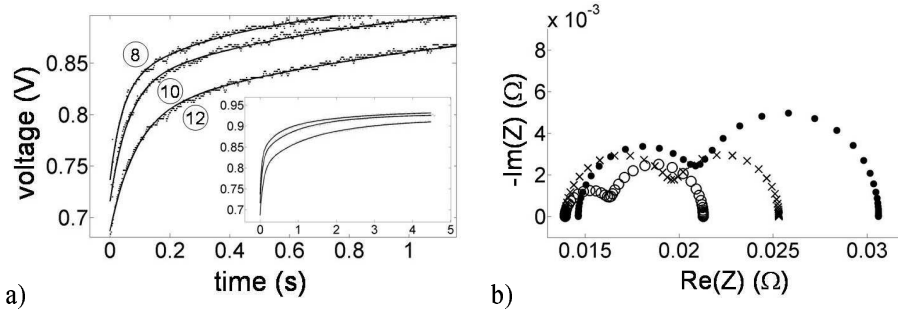

Fig. 8. Results from selected CI runs: a) measured and fitted cell voltages obtained from 8^{th}, 10^{th} and 12^{nd} CI runs; b) impedance spectra calculated from 8^{th} ($\circ$), 10^{th} ($\times$) and 12^{nd} ($\bullet$) CI runs.

7.2 Experiment results

The time evolution of the cell voltage and current are plotted in Fig. 7a and 7b respectively. The voltage and current decrease as time passes, due to the cathode flooding.

As the cathode and the anode exhausts are closed, all the water produced by the electrochemical reaction is accumulated inside the cell. This can be used to estimate the water accumulated inside the cell (χ_{H_2O}) [25]. The initial mass of liquid water inside the cell is zero. Also, the initial cell temperature is low enough to consider that the amount of water in gas phase is negligible.

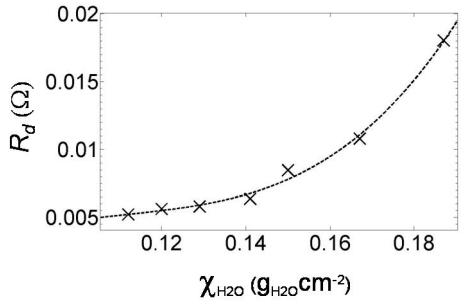

Fig. 9. Diffusion resistance (R_d) vs accumulated amount of water (χ_{H_2O}). Calculated ($\times$), fitted 3^{rd}-order polynomial ($--$)

The method used to estimate the water generated in the cell is discussed in Appendix B. The time evolution of the water accumulated inside the cell is plotted in Fig. 7b.

Several CI runs are performed for different flooding conditions. The measured and fitted cell voltages for the 8^{th}, 10^{th} and 12^{nd} CI runs are shown in Fig. 8a. The corresponding circuit models are calculated by applying the proposed methodology, and they are used to obtain the impedance spectra, which are plotted in Fig. 8b. As expected [14,26], the width of the impedance arcs increases as a result of the cell flooding.

The model parameters calculated from the data of some CI runs, using the Matlab curve fitting toolbox, are shown in Table 2. The parameter SSE is the sum of the quadratic error of the curve fitting.

Note that τ_d, R_d, R_p and C_{dl} depend on the amount of water accumulated inside the cell (χ_{H_2O}). In particular, the diffusion resistance (R_d) depends on the diffusion media coefficient and the oxygen concentration on the active surface (see Eq. (3)). The relationship between R_d and χ_{H_2O} is plotted in Fig. 9. The points calculated from the 7^{th}, 8^{th}, 9^{th}, 10^{th}, 11^{st}, 12^{nd} and 13^{rd} CI runs are represented by the symbol $\times$. The 3^{rd}-order polynomial fitted to

Table 2

PEMFC model parameters calculated for selected CI runs.

CI run	C_{dl} (F)	R_d ($m\Omega$)	R_p ($m\Omega$)	τ_d (s)	R_m ($m\Omega$)	χ_{H_2O} ($g \cdot cm^{-2}$)	SSE
3^{rd}	1.006	4.63	0.50	0.271	14.6	0.037	$0.68 \cdot 10^{-2}$
7^{th}	0.998	5.21	1.59	0.406	13.8	0.112	$0.72 \cdot 10^{-2}$
8^{th}	0.994	5.62	2.01	0.463	13.9	0.120	$1.01 \cdot 10^{-2}$
9^{th}	0.991	5.80	3.88	0.551	10.4	0.129	$1.78 \cdot 10^{-2}$
10^{th}	0.989	6.35	5.30	0.779	13.9	0.141	$1.03 \cdot 10^{-2}$
11^{st}	0.986	8.47	5.54	0.821	12.4	0.150	$1.63 \cdot 10^{-2}$
12^{nd}	0.984	10.8	5.71	0.874	14.6	0.167	$1.06 \cdot 10^{-2}$
13^{rd}	0.973	18.0	6.20	0.947	17.7	0.187	$1.51 \cdot 10^{-2}$

these points is the following:

$$R_d = 25\chi_{\mathrm{H2O}}^3 - 8.3\chi_{\mathrm{H2O}}^2 + 0.96\chi_{\mathrm{H2O}} - 0.033 \tag{26}$$

8 Conclusions

A PEMFC circuit model, well suited for control applications, and a methodology for model parameter estimation from CI data, have been proposed. A key advantage of this approach is that the equipment required to perform the CI tests is easily portable and inexpensive. As a consequence, it can be implemented in cell commercial systems for in-field assessment of the cell. The proposed modelling methodology has been successfully applied to the study

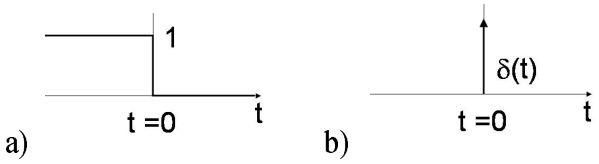

Fig. A.1. Input signals: a) interruption step; and b) unit impulse.

of the cathode flooding phenomenon.

A Interruption step and impulse responses

Consider a plant transfer function described by Eq. (A.1). It will be demonstrated that the plant response to the following two input signals is the same: an interruption step and a unit impulse (see Fig. A.1).

$$F(s) = \sum_i \frac{k_i}{1 + k_i \tau_i s} \qquad \text{where} \begin{cases} k_i, \tau_i \in \Re \\ \\ k_i, \tau_i > 0 \end{cases} \tag{A.1}$$

The plant response to the interruption step can be calculated by subtracting the response to a unit step, $u(t)$, from that to $f(t) = 1$ (i.e., the interruption step can be written as $1 - u(t)$).

The plant response to a unit step is the following:

$$L^{-1}\left[F(s)\frac{1}{s}\right] = L^{-1}\left[\sum_i \frac{k_i}{s\left(1 + k_i \tau_i s\right)}\right] = \sum_i k_i \left(1 - e^{\frac{-t}{k_i \tau_i}}\right) \tag{A.2}$$

The plant response to $f(t) = 1$ is equal to the plant steady-state response to a unit step:

$$\lim_{t\to\infty}\left\{L^{-1}\left[F(s)\frac{1}{s}\right]\right\} = \lim_{s\to 0}\left\{sF(s)\frac{1}{s}\right\} = \lim_{s\to 0}\{F(s)\} = \sum_i k_i \tag{A.3}$$

Therefore, the plant response to an interruption step can be calculated by substracting Eq. (A.2) from Eq. (A.3):

$$\sum_i k_i - \sum_i k_i \left(1 - e^{\frac{-t}{k_i \tau_i}}\right) = \sum_i k_i e^{\frac{-t}{k_i \tau_i}} \tag{A.4}$$

On the other hand, the plant response to a unit impulse is the following:

$$L^{-1}\left[F(s)\right] = L^{-1}\left[\sum_i \frac{k_i}{1 + k_i \tau_i s}\right] = \sum_i k_i e^{\frac{-t}{k_i \tau_i}} \tag{A.5}$$

As Eq. (A.5) is equal to Eq. (A.4), the plant described by Eq. (A.1) has the same response to an interruption step than to a unit impulse.

B Amount of water in the fuel cell

The amount of water ($\Delta\chi_{H_2O}$) generated by electrochemical reaction in the fuel cell during the time period T_m can be calculated from Eq. (B.1). The cell current (I_{ins}), which is supposed constant during that time period, can be calculated from the cell voltage and the load resistance (see Eq. (B.2)).

$$\Delta\chi_{H_2O} = \frac{C_e M_{H_2O} T_m}{S_a N_A n} I_{ins} \tag{B.1}$$

$$I_{ins} = \frac{V_{ins}}{R_{load}} \tag{B.2}$$

After N time intervals, the total amount of water in the cell, $(\chi_{H_2O})_N$, can be calculated from Eq. (B.3), where $(\chi_{H_2O})_0$ is the initial amount water in the cell.

$$(\chi_{H_2O})_N = (\chi_{H_2O})_0 + \sum_{i=1}^{N} (\Delta\chi_{H_2O})_i \tag{B.3}$$

Nomenclature

C_{dl}	Double layer capacitance (F)
C_e	number of electrons in one coulomb (C^{-1})
C_g	Concentration in cathode active layer ($mol \cdot m^{-3}$)
D	Diffusion coefficient ($m^2 \cdot s^{-1}$)
E_{oc}	Open circuit voltage (V)
F	Faraday constant (F)
j	Imaginary unit
M_{H_2O}	Water molar weight ($18.0157 \cdot g \cdot mol^{-1}$)
n	Number of electrons
N_A	Avogadro constant ($6.0221415 \cdot mol^{-1}$)
R	Perfect gas constant ($J \cdot mol^{-1} \cdot K^{-1}$)
R_d	Diffusion resistance (Ω)
R_m	Membrane resistance (Ω)
R_p	Charge transfer resistance (Ω)
s	Laplace transform variable

S Active area (m^2)

S_a Electrode surface (cm^2)

T Temperature (K)

Z_W Warburg

Greek letters

χ_{H_2O} Water load ($g \cdot cm^{-2}$)

δ Diffusion layer width (m)

η_a Anode over-voltage (V)

η_c Cathode over-voltage (V)

η_m Membrane over-voltage (V)

τ_d Diffusion-related time constant (s)

ω Frequency ($rad \cdot s^{-1}$)

References

[1] D.M. Bernardi, M.W. Verbrugge, J. Electrochem. Soc. 139 (1992), 2477-2491.

[2] D. Bevers, M. Wöhr, K. Yasuda, K.Oguro, J. Appl. Electrochem. 27 (1997).

[3] K. Broka, P. Ekdunge, J.Appl. Electrochem. 27 (1997).

[4] J.S. Yi, T.V. Nguyen, J. Electrochem. Soc. 145 (1998), 1149-1159.

[5] V. Gurau, H. Liu, S. Kakac, AIChE J. 44 (1998), 2410-2422.

[6] S. Um, C.Y. Wang, J. Power Sources 125 (2004), 40-51.

[7] A. Rowe, X. Li, J. Power Sources 102 (2001) 82-96.

[8] J. R. Macdonald, Impedance Spectroscopy, John Wiley & Sons, Canada, 1987.

[9] A. G. Hombrados, L. Gonzalez, M. A. Rubio, W. Agila, E. Villanueva, D. Guinea, E. Chimarro, D. Moreno, J.R. Jurado, J. Power Sources, 151 (2005), 25-31.

[10] M. Ciureanu, H. Wang, J. Electrochem. Soc., 146 (11) (1999), 4031-4040.

[11] B. Andreaus, A.J. McEvoy, G.G. Scherer, Electrochem. Acta, 47 (2002), 2223-2229

[12] N. Wagner, J. Applied Electrochem., 32 (2002), 859-863

[13] M. Boillot, C. Bonnet, N. Jatroudakis, P. Carre, S. Didierjean, F. Lapicque, Fuel Cells, 1 (2006), 31-37.

[14] N. Fouquet, C. Doulet, C. Nouillant, G. Dauphin-Tauguy, B. Ould-Bouamama, J. Power Sources, 159 (2005), 905-913

[15] J. Larminie, A. Dicks, Fuel Cell System Explained, John Wiley & Sons, England, 2000.

[16] M. Usman Iftikhar, D. Riu, F. Druart, S. Rosini, Y. Bultel, N. Retiere, J. Power Sources, 160 (2006), 1170-1182.

[17] Jer-Nan Juang, Applied System Identification, PTR Prentice-Hall, New Jersey, 1994.

[18] J.P. Norton, An Introduction of Identification, Academy Press, London, 1986.

[19] K. Ogata, Ingeniera de Control Moderno, Prentice-Hall Hispanoamericana, Mexico, 1985.

[20] R.F. Mann, J.C. Amphlett, M.A.I. Hooper, H.M. Jensen, B.A. Peppley, P.R. Roberge, J. Power Sources, 86 (2000), 173-180.

[21] D. Natarajan, T.V. Nguyen, J. Electrochem. Soc. 148 (2001) A1324A1335.

[22] L. Pisani, G. Murgia, M. Valentini, B. D'Aguanno, J. Power Sources, 108 (2002), 192-203.

[23] I. Sadli, P. Thounthong, J.-P. Martin, S. Raël, B. Davat, J. Power Sources, 156 (2006), 119-125.

[24] T. Mennola, M. Mikkola, M. Noponen, T. Hottinen, P. Lund, J. Power Sources, 112 (2002), 261-272.

[25] M.A. Rubio, W. Agila, A.G. Hombrados, L. Gonzalez, E. Villanueva, J.R. Jurado, D. Guinea, Proceedings XVIII Eurosensors, Rome, 2004.

[26] W. Merida, D.A. Harrington, J.M. Le Canut, G. McLean, J. Power Sources, 161 (2006), 264-274.